Construction and Building Materials 28 (2012) 468–475

Contents lists available at SciVerse ScienceDirect

Construction and Building Materials

journal homepage: www.elsevier.com/locate/conbuildmat

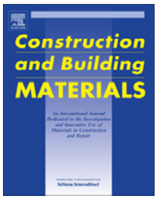

Effect of porosity on thermal expansion coefficient of cement pastes and mortars

Qiang Zeng [a,b], Kefei Li [a,*], Teddy Fen-Chong [b], Patrick Dangla [b]

[a] *Civil Engineering Department, Tsinghua University, Beijing 100084, PR China*
[b] *Université Paris-Est, Laboratoire Navier, Ecole des Ponts ParisTech, LCPC, UMR CNRS, Champs-sur-Marne 77420, France*

ARTICLE INFO

Article history:
Received 1 June 2011
Received in revised form 28 August 2011
Accepted 2 September 2011
Available online 15 November 2011

Keywords:
Thermal expansion coefficient
Cement paste
Mortar
Porosity
Air void

ABSTRACT

The thermal expansion coefficient (TEC) is studied for air-entrained cement pastes and mortars with different porosity. The results show that the porosity has significant effect on the thermal deformation and TEC decreases with porosity. The relation between TEC and porosity observes a power law, $\alpha_d = \alpha_0(1-\phi)^C$, and the exponents C for pastes/mortars are respectively 2.66/2.38 in terms of total porosity, and 3.74/2.69 in terms of air void content. The gravimetry and MIP measurements on the porosity and pore size distribution (PSD) indicate that the entrained air voids have not significant influence on the capillary porosity, but change the PSD curves measured by MIP. Three characteristic pore ranges are identified on these PSD curves and air voids are found to interfere with the mercury intrusion process above the scale of 50 nm. Thermal gravity analysis shows that the composition of hydration products and cement hydration degree for both pastes and mortars are almost the same. The decreased TEC with air-entrainment can probably be attributed to the existence of dense shell structures around the air voids.

1. Introduction

The thermal expansion coefficient (TEC) is one of important thermo-mechanical properties for cement-based materials. It scales the thermal strain of material and the induced thermal stress if the thermal deformation is restraint. Thus, the common practice of concrete technology is to keep the material TEC as low as possible. Furthermore, the TEC of cement paste is of particular interest since it is a fundamental parameter to determine the internal stress among the different phases in cement-based materials and to predict correctly the possible damage induced by the mismatch of thermal dilatation of each phase [1].

Available experimental results show that the typical values for TEC of hardened cement paste are about 15–20 × 10^{-6}/°C [2]. These values are larger than TEC of aggregates, varying from 5 to 12 × 10^{-6}/°C depending on the mineral composition [3]. Cement pastes are typical porous materials with total porosity of 20–40% [4], and the pore water is proved to have a significant influence on the material TEC due to the facts that liquid water has a larger TEC than the solid skeleton of material and that the pore water can accumulate stress during thermal process [5,6]. Under saturated and undrained conditions, the thermal pressurization coefficient, defined as the pore pressure increase per unit temperature rise, of oil well cement paste was estimated to be about 0.6 MPa/°C [7]. The thermal dilatation behavior of liquids confined in small pores has been investigated recently [8,9] and quite important pore pressure was observed by temperature rising [6,7]. Meanwhile, numerous experimental results indicate that, under drained condition, the TEC of saturated samples of cement pastes have almost the same TEC as dried samples [10], and the TEC appears a maximum value at humidity of 65% [11]. Adopting the microstructure model of hydrates by Powers [12], Bazant [13] developed a hydrothermal model for cement paste TEC, decomposing the total thermal dilatation into pure thermal dilation of skeleton, thermal shrinkage (swelling) and hydrothermic dilation of paste. This model was further calibrated by other authors for different moisture conditions [10,14].

Compared to the detailed research on the role of pore water, little attention has been paid to the influence of material porosity on TEC. For most ceramics, it is reported that the TEC is independent of porosity [15]. However, the porosity of ceramics is controlled, in industry, to fabricate the low TEC materials. For instance, the cordierite ceramics were sintered with porosity about 40% to obtain a TEC as low as 0.4 × 10^{-6}/°C [16]. For cement-based materials, Shui et al. [17] showed that the TEC decreased with the increase of material porosity and explained that this decrease was due to the pores accommodating a part of the internal thermal expansion of solid skeleton. This argument was further supported by other experimental observations [18]. However, based on the poromechanics analysis, Ghabezloo obtained the opposite conclusion [19]. Thus, more research is needed to understand the mechanism of porosity's impact on TEC. To this aim, the TEC of cement pastes and mortars with different porosities are investigated in this paper. The temperature range of TEC measurement is −35 to 15 °C, an usual range for atmospheric exposure of engineering cement-based materials. The

---

[*] Corresponding author.
E-mail address: likefei@tsinghua.edu.cn (K. Li).

0950-0618/$ - see front matter © 2011 Elsevier Ltd. All rights reserved.
doi:10.1016/j.conbuildmat.2011.09.010

mercury intrusion porosimetry (MIP) and the thermal gravity analysis (TGA) were performed to characterize the pore structure and hydration products respectively. On the basis of the measurements, the role of porosity on TEC is discussed in depth.

2. Theoretical basis

Several available models for TEC of porous media are recalled here to provide a theoretical basis for interpreting the experimental data later in this paper. For sintered porous metals, the TEC relates intimately to the porosity [20] through a power law,

$$\alpha_d = \alpha_s \rho^{1/3} = \alpha_s (1-\phi)^{1/3} \tag{1}$$

where α_d is the TEC of porous material, α_s is the TEC of solid skeleton, ρ is the relative density between porous material and its solid skeleton. From this law, the increase of porosity leads to the decrease of material TEC. A general composite model expresses the material TEC as the volume average of skeleton TEC and pore phase TEC [21],

$$\alpha_d = \alpha_s (1-\phi) + \alpha_p \phi \tag{2}$$

where α_p is the TEC of pore (filling) phase. As the pores are totally dried the pore filling phase is air, and the thermal dilatations of air phase and solid skeleton are no more compatible thus this expression is no longer valid. Ghabezloo [19] gave a poroelastic description of thermal deformation of porous material and derived the differential of TEC with respect to porosity as,

$$\frac{\partial \alpha_d}{\partial \phi} = -\frac{1}{K_d^2}\left[\frac{1-\phi}{K_d} - \frac{1}{K_s}\right]^{-1} \frac{\partial K_d}{\partial T} \tag{3}$$

where K_d is the drained bulk modulus of porous material, and K_s the unjacked bulk modulus or the bulk modulus of solid matrix. The detailed derivation of equations is given in Appendix A, see also [22]. The experimental results by Odelson et al. [23] show that the undrained bulk modulus decreases with temperature, i.e. $\partial K_d/\partial T < 0$. The term $-1/K_d^2[(1-\phi)/K_d - 1/K_s]^{-1}$ is negative too since the term $1-\phi > K_d/K_s$ holds for most cement-based materials, e.g. Ghabezloo measured $K_d/K_s = 0.414$ and $1-\phi = 0.74$ for oil-well cement pastes [7]. Accordingly, it is stated that the TEC of cement-based materials, in drained condition, increases with porosity [19]. It is to note that if the drained bulk modulus K_d is regarded as independent on temperature, i.e. $\partial K_d/\partial T = 0$, then Eq. (3) depicts a simple fact that,

$$\frac{\partial \alpha_d}{\partial \phi} = 0: \quad \alpha_d = \alpha_d(\phi = 0) = \alpha_s \tag{4}$$

In fact, Khalili et al. [24] provide the proof of this relation from a boundary value problem in classic poromechanics with the matrix drained modulus independent on temperature.

3. Experiments

3.1. Materials

A type of Portland cement supplied by Larfage was used in the study. The chemical composition and physical properties of cement are given in Table 1. The mineral contents of cement were analyzed, through Bogue's procedure, as C_2S (21.38%), C_3S (58.88%), C_3A (6.49%), C_4AF (8.77%), Gypsum (0.75%) and others (3.73%). This cement corresponds to CEM I type according to European standard [25].

3.2. Sample preparation

Table 1
Chemical composition and physical properties of cement.

Chemical composition/physical properties	Cement
Silica (Si_2)	22.93
Alumina (Al_2O_3)	4.29
Iron oxide (Fe_2O_3)	2.89
Calcium oxide (CaO)	66.23
Magnesium oxide (MgO)	1.92
Sulfur trioxide (SO_3)	0.35
Sodium oxide (Na_2O (eq))	0.70
Free calcium oxide (CaO (f))	0.64
Chloride (Cl)	0.006
Loss on ignition (LOI)	1.70
Density (g/ml)	3.12
Specific area (m^2/kg)	343

Cement pastes and mortars were prepared with w/c = 0.5. For mortars, the sand–cement ratio was retained as 2.25 and the modulus of sands is 2.5. Air entrainment agent (AEA) was added, in four dosages, into the cement paste and mortar mixtures to create different porosities in hardened samples. Note P (M)-*i* the paste (mortar) sample with *i* = 0, 1, 2, 3, 4 standing for the dosage, AEA mass versus cement mass, of 30, 60, 90 and 120 μg/g respectively. After mixing cement pastes and mortars were cast into cylinder tubes of 10 mm diameter and the hardened specimens were demoulded from the tubes at 3 d, then immersed into saturate lime-water.

The samples with curing age of 300 d were taken out from lime-water and weighted as M_0. The samples were then oven-dried at 50 °C to constant weight M_d. This temperature is regarded as capable to avoid the possible drying damage in samples [26]. The normalized weight loss in drying process of pastes and mortars were present in Fig. 1. The weight for all samples reached nearly constant after drying of 60 h. For each material, the dried samples were divided into three groups. The first group were kept in desiccator for the thermal dilation measurement, and the second dried group of samples were vacuum-saturated with water. The outlet gas pressure was controlled to under 0.1 atm, and the vacuum-saturation last 48 h to guarantee the saturation of the air voids as well. The vacuum-saturated samples were weighted as M_s. The last group of dried samples were then ground into small particles to perform helium pycnometry (HP), mercury intrusion porosimetry (MIP) and thermal gravity analysis (TGA).

3.3. Porosity and air void content

By the gravimetry method mentioned above, the capillary porosity ϕ_m and the air-void content ϕ_av, for each material, are obtained through weight measurement:

$$\phi_m = \frac{(M_0 - M_d)/\rho_w}{M_d/\rho_s} \tag{5a}$$

$$\phi_\mathrm{av} = \frac{(M_s - M_d)/\rho_w - (M_0 - M_d)/\rho_w}{M_d/\rho_s} \tag{5b}$$

where ρ_w is the density of pore liquid ($\rho_w = 0.997$ kg/m^3 for water) and ρ_s is the skeleton density which can be measured by helium pycnometry (HP) or mercury intrusion porosimetry (MIP). The analysis results are given in Table 2.

3.4. MIP measurement

The MIP measurement is based on the principle that the intrusion volume of mercury into a porous medium depends on the applied pressure. Following the assumption that the pore geometry is cylindrical, the pore diameter (size) d can be expressed in terms of pressure P through Washburn equation,